JHEP HYPER VERSION

Received: *August 11, 2001*, Accepted: *October 1, 2001*
Revised: *September 25, 2001*

Exploring neutrino mixing with low energy superbeams

Hisakazu Minakata

Department of Physics, Tokyo Metropolitan University
1-1 Minami-Osawa, Hachioji, Tokyo 192-0397, Japan
E-mail: minakata@phys.metro-u.ac.jp

Hiroshi Nunokawa*

Instituto de Física Gleb Wataghin, Universidade Estadual de Campinas - UNICAMP, P.O. Box 6165, 13083-970 Campinas SP Brazil
E-mail: nunokawa@ifi.unicamp.br

Abstract: We explore the features of neutrino oscillation which are relevant for measurements of the leptonic CP violating phase δ and the sign of Δm^2_{13} in experiments with low-energy conventional superbeams. Toward the goal, we introduce a new powerful tool called the "CP trajectory diagram in bi-probability space" which allows us to represent pictorially the three effects, the effects of (a) genuine CP violation due to the $\sin\delta$ term, (b) CP conserving $\cos\delta$ term, and (c) fake CP violation due to earth matter, separately in a single diagram. By using the diagram, we observe that there is a two-fold ambiguity in the determination of δ which is related with the sign of Δm^2_{13}. Possible ways of resolving the ambiguity are discussed. In particular, we point out that an in situ simultaneous measurement of δ and the sign of Δm^2_{13} can be carried out at distances of about 700 km, or at the Phase II of the JHF experiment provided that $\sin\delta \cdot \Delta m^2_{13} < 0$, both with a megaton class water Cherenkov detector.

Keywords: Solar and Atmospheric Neutrinos, Neutrino Physics, CP violation.

*Present address: Instituto de Física Teórica Universidade Estadual Paulista Rua Pamplona 145 01405-900 São Paulo, SP Brazil E-mail: nunokawa@ift.unesp.br

JHEP10(2001)001

Contents

1. Introduction **1**

2. Matter effect helps to resolve two-fold ambiguity in vacuum neutrino oscillation **4**

3. CP trajectory diagram in bi-probability space **6**

4. Principle of choosing beam energies for long-baseline neutrino oscillation experiments **10**

5. Resolving two-fold ambiguity in determination of δ **12**

5.1 Chance for simultaneous measurement of δ and the sign of Δm^2_{13} in situ 12

5.2 Two-detector method 12

6. Long-baseline neutrino oscillation experiments with superbeams; some concrete examples **16**

6.1 Method for calculation of number of events 17

6.2 Single detector at $L = 300\,\mathrm{km}$ 18

6.3 Single detector at $L = 700/1000\,\mathrm{km}$ 21

6.4 Two detectors at $L = 300$ and $700/1000\,\mathrm{km}$ 23

7. CP trajectory diagram for neutrino factories **23**

8. Conclusion **24**

A. Proof of ellipticity of CP trajectory diagram **26**

1. Introduction

Discovery of neutrino oscillation in atmospheric neutrino observation in the Super-Kamiokande (SK) experiment [1] opened up a new window to physics beyond the standard model of particle physics. Moreover, robust discrepancy of the measured flux of solar neutrinos to the calculated one [2] presents another indication for neutrino masses and the lepton flavor mixing. In fact, the first result from the SNO [3] group combined with the results by the Super-Kamiokande solar neutrino observation [4] strongly indicates that solar neutrinos also do oscillate. The existence

JHEP10(2001)001

of phenomenon of neutrino oscillation is further strengthened by the result of the K2K experiment, the first long-baseline experiment with artificial neutrino beam, in particular by their latest result [5].

The determination of the complete structure of the lepton flavor mixing matrix, the Maki-Nakagawa-Sakata (MNS) matrix [6], is one of the most challenging task in particle physics. While we began to grasp the values of the leptonic mixing parameters there remain three quantities which are poorly known or not constrained at all at this moment. They are θ_{13}, the sign of Δm^2_{13}, and δ, the leptonic Kobayashi-Maskawa angle [7, 8]. (See e.g. ref. [9] for a summary of situations of yet to be determined parameters in the three-flavor mixing scheme of neutrinos.) Regarding to θ_{13}, we only know its upper limit, $\sin^2 2\theta_{13} \lesssim 0.1$, from the reactor experiments [10]. The bound is to be improved, or the value of θ_{13} itself could be determined by the next generation long baseline experiments [11, 12, 13]. About the sign of Δm^2_{13}, while there is a strong indication that the inverted mass hierarchy (or negative Δm^2_{13}) is disfavored by the observed neutrino events coming from supernova SN1987A [14], no hint is available from laboratory experiments. With respect to CP phase, δ, we do not have any experimental clue at all.

In this paper, we intend to explore as clearly as possible the features of neutrino oscillation which are relevant for experimental measurements of the latter two quantities, δ and the sign of Δm^2_{13}. We focus on the so called low-energy option [9] and discuss principles for optimizing experimental parameters to measure these two quantities simultaneously. Toward the goal, we first formulate a method for obtaining a bird-eye view of the phenomenon of neutrino oscillation at low neutrino energies, typically, 0.5-2.0 GeV. We do this by introducing a new powerful tool called the "CP trajectory diagram in bi-probability space", which allows us to represent pictorially the effects of genuine CP violating phase and the earth matter [15] separately in a single diagram, as explained in detail below. We then address the question of what are the promising options for conceptual design of experiments which look for CP violation among thinkable varying possibilities at low energies.

We have discussed in previous communications [16, 17] the possibility of use of an intense low energy neutrino beam, which is nowadays referred to as a "superbeam" à la Richter [18], to measure CP violation. It is based on the underlying cancellation mechanism of the leading-order matter effect, the vacuum mimicking mechanism [19], which would allow us to measure CP violation in a clean vacuum-effect-dominated environment for neutrino oscillations. It gives us a great merit of avoiding the notorious problem of matter effect contamination [20]–[23].

As a concrete example which realizes our basic idea we designed and examined an experiment which uses a neutrino superbeam of energy $E \simeq 100\,\mathrm{MeV}$ and a 1 megaton water Cherenkov detector [16, 17]. We have ended up with a rather short baseline, $L \sim 30 - 40\,\mathrm{km}$, as optimal distance in such an experiment. While it served well for our purpose of illuminating the basic idea, several experimental problems

JHEP10(2001)001

have been raised when it was taken at face value as an experimental proposal. (See, however, [24] for a detailed feasibility study of the very similar idea, $E = 250\,\mathrm{MeV}$, $L \sim 100\,\mathrm{km}$, and a 40 kton water Cherenkov or liquid scintillator detectors.)

If we simply scale up the energy range to the more realistic one, $E \sim 1\,\mathrm{GeV}$, keeping E/L fixed as in ref. [16, 17], the optimal distance may become naively $L \sim$ 300-400 km. It is very similar to the experimental set up recently discussed by the JHF neutrino experimentalists. In particular, by the JHF neutrino working group, various options for neutrino beam, wide band (WB) beam, narrow band (NB) beam, and off-axis (OA) beam with neutrino energies of 500 MeV-a few GeV have been extensively studied [25]. Moreover, the efficiency of removing π^0 contamination has been improved tremendously since the old Letter of Intent (LOI) [11] by implementing severe cut by imposing a second ring, a new technique originally developed by the Super-Kamiokande group [26]. See their new version of LOI in [27].

In this paper we try to make a step forward along the line of thought toward measuring CP violation with use of low energy conventional superbeam by describing a general strategy of optimizing beam energy and/or baseline distance. We will show that the matter effect are comfortably large even in these mediumly long baseline ($\sim 300\,\mathrm{km}$) experiments so that there is a possibility of simultaneous measurement of δ, the leptonic Kobayashi-Maskawa angle, and the sign of Δm^2_{atm} in situ in a single experiment.

An alternative strategy based on intense neutrino beam from a muon storage ring called neutrino factory has been extensively discussed in the literature [28, 29].[1] Our strategy which utilizes low energy conventional superbeam differs in many ways from neutrino factory, e.g., on beam energy, detection principle, and on whether the value of θ_{13} is expected to be known in advance (which we assume for conventional beam in this paper), or can be measured simultaneously with δ (neutrino factory). While many discussions are going on upon ignition by ref. [18] about which strategy is more superior [30], we strongly feel that both strategies must be fully developed both in physics and beam technology aspects before attempting any real comparisons between the two strategies.

The motivation for our consideration of neutrino experiments with beam energies of $\sim 1\,\mathrm{GeV}$ in this paper is partly theoretical and partly experimental. Experimentally, the energy region comes out as a natural compromise of the two requests that CP violation is large and neutrino beam is intense enough. Furthermore, it has a great merit of being able to utilize the results of the recent developments we just mentioned above. On the theoretical side, we discuss below by using the "CP trajectory diagram" a principle of optimizing beam energy and/or path length to maximizes the detection probability of CP violation. We will see that such discussion naturally

[1] A neutrino factory version of low energy experiment is discussed by M. Koike and J. Sato in ref. [23].

JHEP10(2001)001

leads to several options which utilize the same energy region, $E \sim 1\,\mathrm{GeV}$. Notably, we will uncover the possibility in which an in situ simultaneous measurement of CP violating phase δ and the sign of Δm^2_{13} will be possible for (i) whole region of δ ($L \simeq 700\,\mathrm{km}$), and (ii) half a region of δ which fulfills the condition $\sin\delta \cdot \Delta m^2_{13} < 0$ ($L \simeq 300\,\mathrm{km}$).

In section 2 we point out that an approximate two-fold degeneracy exists in vacuum neutrino oscillation probability and show that the degeneracy is partly lifted by the matter effect. We introduce in section 3 the CP trajectory diagram on bi-probability space, and thoroughly analyze its properties. It will be shown that it is a powerful tool for illuminating the general structure of the oscillation probabilities of neutrinos and antineutrinos. We will point out that the two-fold degeneracy which exists in vacuum neutrino oscillation probability, after resolved by matter effect, leaves a remnant ambiguity in the determination of CP violating phase δ. We then discuss in section 4 a principle of tuning beam energies to have maximal CP violation as well as to help in resolving the two-fold ambiguity. In section 5 we describe several possible ideas for resolving the two-fold ambiguity. Throughout these sections we will reveal that a new strategy toward simultaneous determination of the CP violating angle δ and the sign of Δm^2_{13} naturally emerges from the discussions of problems mentioned above. In section 6 we describe some concrete examples of experiments which utilize conventional neutrino superbeams. We estimate the number of events and include the background rate to obtain a rough idea for the accuracy of the measurement. In section 7 we briefly discuss the CP trajectory diagram with experimental parameters for neutrino factory. In section 8 we state our conclusions.

2. Matter effect helps to resolve two-fold ambiguity in vacuum neutrino oscillation

We start by describing a role played by matter effect to help resolve a two-fold ambiguity which would exist in a vacuum-effect dominated neutrino oscillation experiment to measure CP violating angle δ. It contrasts to the negative role played by the matter effect as a contamination in measurement of genuine CP violation, the widely recognized fact in the literature [20]–[23]. We hope that the discussion illuminates the necessity of complete understanding of the interplay between effects due to the Kobayashi-Maskawa phase and earth matter.

We use throughout this paper the standard notation of the MNS matrix:

$$U = \begin{bmatrix} c_{12}c_{13} & s_{12}c_{13} & s_{13}e^{-i\delta} \\ -s_{12}c_{23} - c_{12}s_{23}s_{13}e^{i\delta} & c_{12}c_{23} - s_{12}s_{23}s_{13}e^{i\delta} & s_{23}c_{13} \\ s_{12}s_{23} - c_{12}c_{23}s_{13}e^{i\delta} & -c_{12}s_{23} - s_{12}c_{23}s_{13}e^{i\delta} & c_{23}c_{13} \end{bmatrix}. \qquad (2.1)$$

JHEP10(2001)001

We define the neutrino mass-squared difference as $\Delta m^2_{ij} \equiv m^2_j - m^2_i$ where Δm^2_{12} is assumed to be smallest, relevant for oscillation solutions to the solar neutrino problem. We note in passing that in the MSW mechanism, under the assumption that $\Delta m^2_{23} \sim \Delta m^2_{13}$ is much larger than Δm^2_{12}, latter can be made always positive as far as θ_{12} is taken in its full range $[0,\, \pi/2]$[31].

The ambiguity arises due to the fact that Δm^2 scale implied by solar neutrino solution may be small such that

$$\frac{\Delta m^2_{12} L}{2E} = 2.54 \times 10^{-2} \left(\frac{\Delta m^2_{12}}{10^{-5}\ \mathrm{eV}^2}\right) \left(\frac{L}{1000\ \mathrm{km}}\right) \left(\frac{E}{1\ \mathrm{GeV}}\right)^{-1} \tag{2.2}$$

is sufficiently small compared to unity for most of the possible experimental parameters. To first order in the parameter the neutrino oscillation probabilities of $\nu_\mu \to \nu_e$ and $\bar{\nu}_\mu \to \bar{\nu}_e$ in vacuum are given by

$$\begin{aligned} P_{vac\pm}[\nu_\mu(\bar{\nu}_\mu) \to \nu_{\mathrm{e}}(\bar{\nu}_e)] = {} & \sin^2 2\theta_{13} s^2_{23} \sin^2 \left(\frac{\Delta m^2_{13} L}{4E}\right) - \\ & -\frac{1}{2} s^2_{12} \sin^2 2\theta_{13} s^2_{23} \left(\frac{\Delta m^2_{12} L}{2E}\right) \sin \left(\frac{\Delta m^2_{13} L}{2E}\right) + \\ & +2 J_r \cos\delta \left(\frac{\Delta m^2_{12} L}{2E}\right) \sin \left(\frac{\Delta m^2_{13} L}{2E}\right) \mp \\ & \mp 4 J_r \sin\delta \left(\frac{\Delta m^2_{12} L}{2E}\right) \sin^2 \left(\frac{\Delta m^2_{13} L}{4E}\right), \end{aligned} \tag{2.3}$$

where $-$ and $+$ sign in front of the 4th term refer to the neutrino and the antineutrino channels, respectively, and $J_r = c_{12} s_{12} c^2_{13} s_{13} c_{23} s_{23}$ denotes the reduced Jarlskog factor. One can readily observe that the oscillation probabilities, except for the second term, are invariant under simultaneous transformation

$$\begin{aligned} & \delta \to \pi - \delta \qquad (\mathrm{mod}\ 2\pi), \\ & \Delta m^2_{13} \to -\Delta m^2_{13}\,. \end{aligned} \tag{2.4}$$

Under the transformation (2.4), flipping sign of the $\cos\delta$ term by the first transformation is canceled by the second, whereas the $\sin\delta$ term is manifestly invariant. It implies that the probability is approximately degenerate for two values of δ, unless one know a priori the sign of Δm^2_{13}, and hence there is a two-fold ambiguity in determination of δ.

We note that the invariance holds in a very good approximation. It is because the second term is small in magnitude because of the suppression factors including $(\Delta m^2_{12} L/2E)$ and the fact that $\sin^2 2\theta_{13}$ is smaller than 0.1 in order to satisfy the CHOOZ result [10]. Also the higher order terms of $(\Delta m^2_{12} L/2E)$ is sufficiently small for most of the experimental settings. It may be worthwhile, however, to note that the degeneracy is accidental and approximate in nature, and represents neither inherent nor exact properties of vacuum neutrino oscillations.

JHEP10(2001)001

Of course, the ambiguity does not exist if we know in advance the sign of Δm^2_{13}. However, it is very unlikely that the question of the normal vs. inverted mass hierarchies of neutrinos will be answered in a convincing way in the near future. It is because (as it is believed) the determination of the sign of Δm^2_{13} requires measurement of interference between the CP and the matter effects, which necessitates a sufficiently long baseline. It is not an easy experiment to carry out because it requires either intense neutrino beam or supermassive detectors, or plausibly both.

We now point out that the two-fold degeneracy in vacuum oscillation probability is lifted by the matter effect represented by the index of refraction $a(x) = \sqrt{2}G_F N_e(x)$ where G_F is the Fermi constant and $N_e(x)$ denotes the electron number density at x in the earth. When we include the matter effect there arise, in leading order of aL, the following additional terms $P_{\rm matt}$ in the oscillation probability computed under the adiabatic approximation [20]:

$$P_{\rm matt\pm}[\nu_\mu(\bar{\nu}_\mu) \to \nu_{\rm e}(\bar{\nu}_e)] = \pm \cos 2\theta_{13} \sin^2 2\theta_{13} s^2_{23} \left(\frac{2Ea(x)}{\Delta m^2_{13}}\right) \sin^2\left(\frac{\Delta m^2_{13} L}{4E}\right) \mp$$
$$\mp \frac{a(x)L}{4} \sin^2 2\theta_{13} \cos 2\theta_{13} s^2_{23} \sin\left(\frac{\Delta m^2_{13} L}{2E}\right), \qquad (2.5)$$

In (2.5), $+(-)$ in the 1st term and $-(+)$ in the 2nd term refer to the neutrino (antineutrino) channel.

It is easy to observe that the degeneracy is lifted because $P_{\rm matt}$ is not invariant under flipping sign of Δm^2_{13}, a well known fact. What is perhaps not so well known is that the lifting of the degeneracy does not completely resolve the two-fold ambiguity in determination of δ. We introduce in the next section a powerful tool called the "CP trajectory diagram" and demonstrate that a remnant ambiguity exists in the determination of CP violating phase. Since the ambiguity is related with the sign of Δm^2_{13}, we are naturally invited to the problem of simultaneous determination of δ and the sign of Δm^2_{13}, which we will pursue in section 6.

3. CP trajectory diagram in bi-probability space

To illuminate global features of neutrino oscillations relevant for low energy experiments, we introduce the CP trajectory diagram in bi-probability space spanned by $P(\nu)$ and $P(\bar{\nu})$ [32]. Unless otherwise stated we simply denote $P(\nu_\mu \to \nu_e)$ and $P(\bar{\nu}_\mu \to \bar{\nu}_e)$ as $P(\nu)$ and $P(\bar{\nu})$ in this paper. We show in this section that the diagram is a useful tool for our purpose because it can display pictorially the three effects separately in a single diagram; genuine effect of CP violating phase δ coming from $\sin\delta$ term, CP conserving effect due to $\cos\delta$ term, and the matter effect.

Suppose that we compute the oscillation probability $P(\nu)$ and $P(\bar{\nu})$ with a given set of oscillation and experimental parameters. Then, we draw a dot on two-

JHEP10(2001)001

dimensional plane spanned by $P(\nu)$ and $P(\bar{\nu})$. When δ is varied we have a set of dots which forms a closed trajectory, closed because the probability must be a periodic function of δ, a phase variable.

In figure 1 plotted is the contours of oscillation probabilities $P(\nu)$ and $P(\bar{\nu})$ which are drawn by varying the CP violating phase, δ, from 0 to 2π. We note that in this work, while we refer to analytic expressions for the explanations, all the results shown in our plots as well as in tables were based on the computations obtained by numerically solving the three flavor neutrino evolution equation assuming constant matter density. The solid and the dashed lines are for positive and negative Δm^2_{13}, respectively. The dotted and the dash-dotted curves are the cases in vacuum in which the matter effect is switched off in the corresponding cases of the solid and the dashed lines, respectively. In fact, the abscissa and the ordinate are not quite the oscillation probabilities but are the ones averaged over an appropriate energy distribution of (anti-) neutrinos. It is to avoid accidental zeros, and at the same time is also meant to mimic the average over the energy dependent flux times cross sections, the procedure we will actually execute in section 6. The neutrino energy distribution is taken to be a Gaussian shape with central value of (a) 0.5 GeV, (b) 1.0 GeV, (c) 1.5 GeV, and (d) 2.0 GeV, respectively. The widths of Gaussian distribution is taken to be 20 % of the peak energies, e.g., 100 MeV for $E = 500$ MeV in figure 1*a*. The baseline length is taken to be 295 km, JHF-Kamioka distance, and the values of other parameters are typical ones for the large angle MSW solution to the solar neutrino problem and $\sin^2 2\theta_{13} = 0.05$, as given in the caption of figure 1. Notice that unless the large angle MSW solution is the case the measurement of CP violation would be very difficult.

As one might have suspected by looking in figure 1 the CP trajectory is elliptic. It is easy to prove it in the vacuum case and it can be also shown that it is the case in a good approximation for oscillations in matter. The proof of the statements will be given in Appendix. In particular, it is shown that the major (or minor) axis is always at 45 degree in the vacuum case.

What does CP trajectory diagram actually represent? To answer the question, we start with the vacuum case and first concentrate on figure 1*a*–*c*. In these cases, the lengths of the major and the minor axes are measures for the coefficients of $\sin\delta$ and $\cos\delta$, respectively, in the oscillation probability. (The same statement holds for figure 1*d* if the major and the minor axes are interchanged.) One can readily understand this statement by looking at eq. (A.3) in Appendix.

The two trajectories of positive and negative Δm^2_{13} which are represented by dotted and the dash-dotted lines, respectively, are almost degenerate. One notices that the approximate degeneracy is between δ and $\pi - \delta$ (mod. $2\ \pi$) cases as we anticipated in discussions in the previous section. The two trajectories slightly split mainly due to the second term in eq. (2.3) and possibly by higher order terms of $(\Delta m^2_{12} L/2E)$ which are not taken into account in eq. (2.3).

JHEP10(2001)001

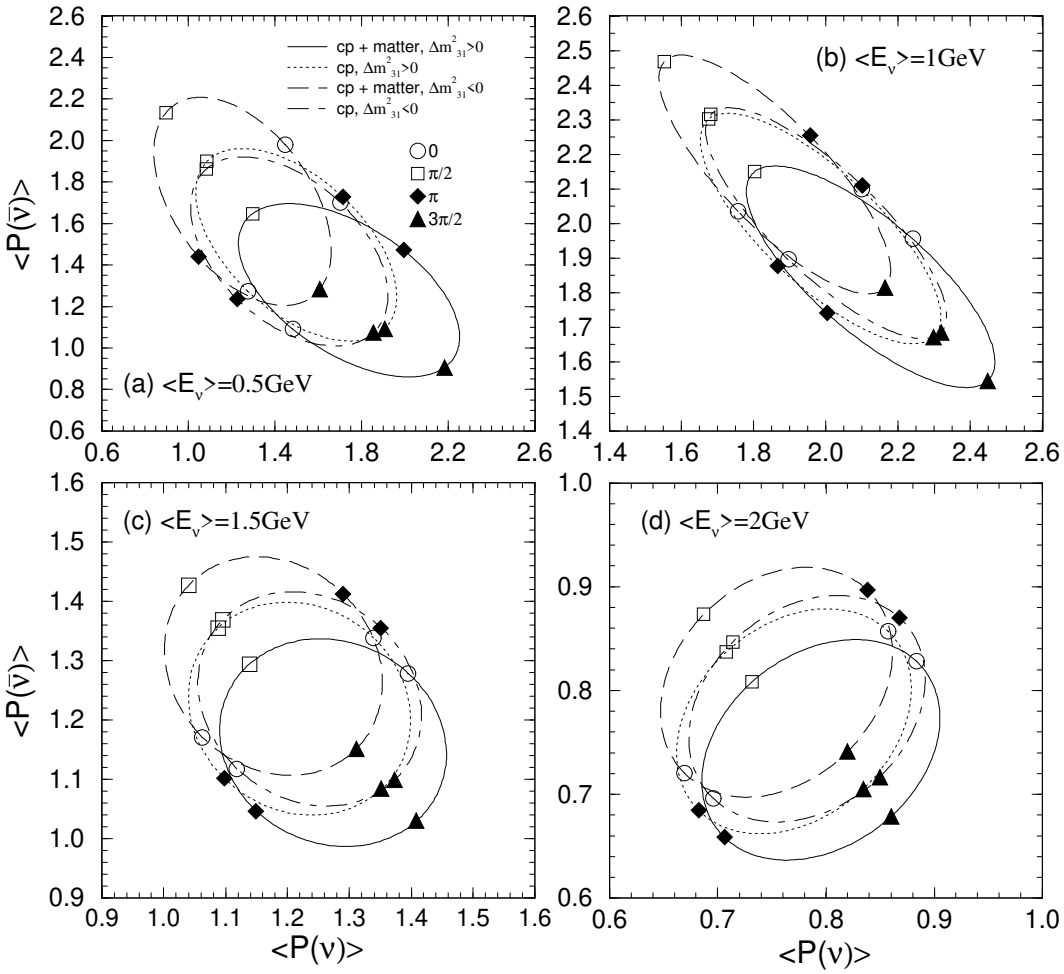

Figure 1: CP trajectory in the bi-probability (given in %) plane for the baseline $L = 295$ km. As indicated in the figures, the solid and the dashed lines are for $\Delta m^2_{13} > 0$ and $\Delta m^2_{13} < 0$ cases, respectively, and the dotted and the dash-dotted lines correspond to the same signs of Δm^2_{13} as above but with matter effect switched off. The mixing parameters are fixed as $\Delta m^2_{13} = \pm 3 \times 10^{-3}$ eV^2, $\sin^2 2\theta_{23} = 1.0$, $\Delta m^2_{12} = 5 \times 10^{-5}$ eV^2, $\sin^2 2\theta_{12} = 0.8$, $\sin^2 2\theta_{13} = 0.05$. We take $\rho Y_e = 1.4$ g/cm^3 where ρ is the matter density and Y_e is the electron fraction.

In matter, the CP trajectories of neutrinos and antineutrinos split; the former moves to downward-right ($\Delta m^2_{13} > 0$) and the latter to upward-left ($\Delta m^2_{13} < 0$). In fact, one can explicitly demonstrate that the matter effect is the cause of the departure of the two trajectories by artificially increasing the matter potential a. In figure 2, presented are the results of the same computations as in figure 1 but with a factor of 2 (artificially) larger matter effect. One observes that the neutrino and the antineutrino trajectories became more separated along the direction of major (minor) axis on bi-probability plane in figure 2*a–c* (figure 2*d*). Therefore, the degree of nonoverlapping of neutrino and antineutrino trajectories gives almost purely the measure for the matter effect.

JHEP10(2001)001

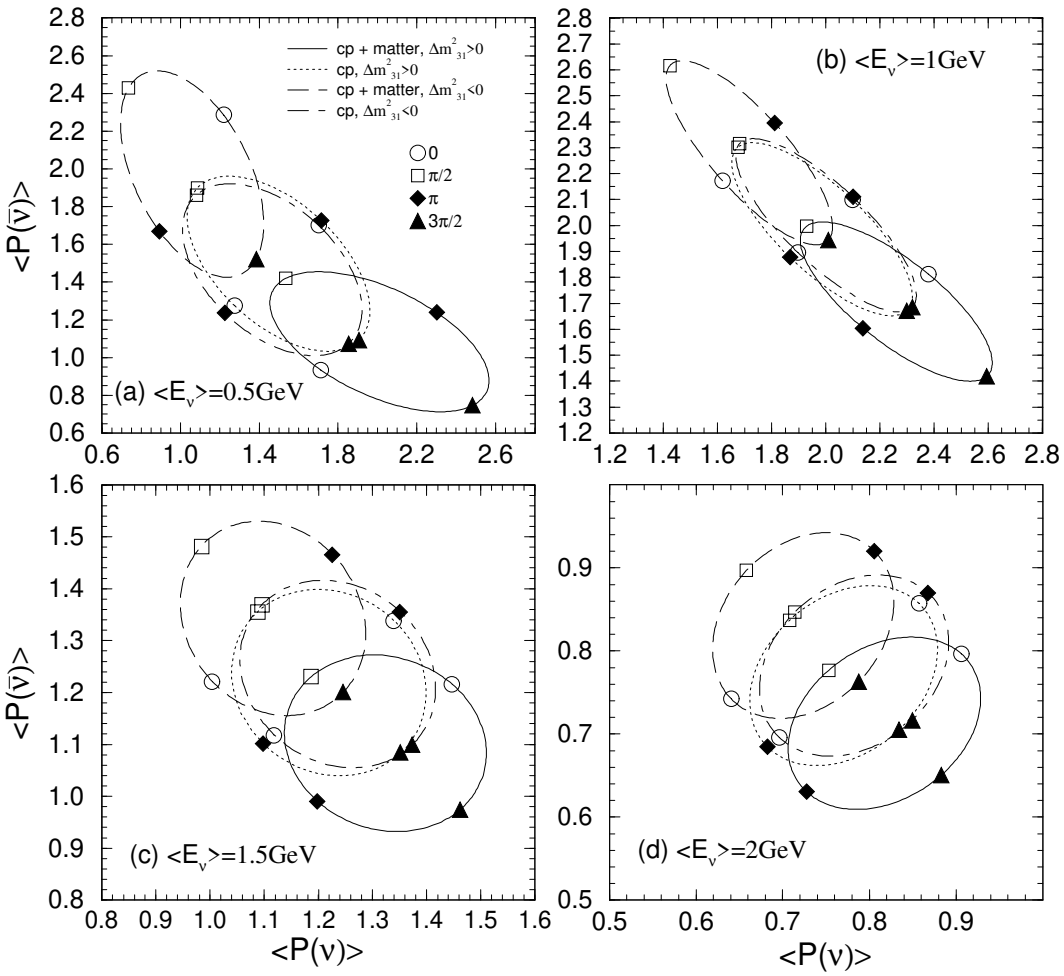

Figure 2: The same as in figure 2 but for $\rho Y_e = 2.8\,\mathrm{g/cm^3}$.

It is important to notice, by comparing the cases in vacuum and in matter in each figure, that lengths of the major and the minor axes, which measure the effect of $\sin\delta$ term, the genuine CP violation, and the $\cos\delta$ term, respectively, barely change by the matter effect. It is nothing but the feature which we expect from the perturbative formula in eqs. (2.3) and (2.5).

Thus, the matter effect lifts the two-fold degeneracy of δ and $\pi - \delta$ cases discussed in section 2, as shown in figure 1. Notice, however, that there still remains two crossing points of the two trajectories corresponding to positive and negative Δm^2_{13} as indicated in figure 1. It means that if we are unlucky so that the true value of δ is close to the crossing point, then we will still have two-fold degeneracy in determination of δ. Since we expect only a modest statistics even with a huge detector in experiments for measuring δ, the region suffered by the ambiguity problem may not be so small, unless nature was so kind to tune her parameters to produce maximal CP violating effects. We will discuss in the next section how to resolve the remaining two-fold ambiguity.

JHEP10(2001)001

We emphasize that it is one of the nicest features of the CP trajectory diagram that the CP violating as well as conserving effects due to the Kobayashi-Maskawa phase, and the earth matter effect are pictorially displayed separately in a single diagram.

The readers may worry about the apparently intricate features of the CP trajectory diagram indicated in figures 1 and 2. They include:

(F1) the feature that the "chirality" of the trajectory depends upon the sign of Δm^2_{13}. Here, what we mean by "chirality" is how a trajectory winds, clockwise or counter-clockwise, as δ varies from 0 to 2π.

(F2) the dependence on the neutrino energy; between energies of 0.5 GeV and 1 GeV the positions of $\delta = 0$ and $\delta = \pi$ are exchanged completely. At the same time, the "chirality" of the trajectory also flips from 0.5 GeV to 1 GeV.

The explanation of (F1) and (F2) are in fact very simple.

(A1) Since the δ-development of the trajectory is uniform, it suffices to discuss the behavior of the trajectory at around $\delta = 0$. When δ increases from zero, the $\sin\delta$ term in the oscillation probability (2.3) decreases (increases) in neutrino (antineutrino) channel. This means that the movement of the trajectory is toward upward-left direction for both $\Delta m^2_{13} > 0$ and $\Delta m^2_{13} < 0$ cases.

The trajectory winds in opposite way for positive and negative Δm^2_{13} because the point $\delta = 0$ is located at near (far) side from the origin for $\Delta m^2_{13} > 0$ ($\Delta m^2_{13} < 0$) case, due to the $\cos\delta$ term in the probability (2.3), at $E = 0.5\,\mathrm{GeV}$ as in figure 1*a*. It means that the trajectory winds clockwise for $\Delta m^2_{13} > 0$ and winds counter-clockwise for $\Delta m^2_{13} < 0$.

(A2) When neutrino energy increases from $E = 0.5\,\mathrm{GeV}$ to 1 GeV, $\sin(\Delta m^2_{13} L/2E)$ changes sign from negative to positive at $L = 300\,\mathrm{km}$. Then, the $\cos\delta$ term flips the sign and the $\delta = 0$ point jumps to the far (near) side of the trajectory in $\Delta m^2_{13} > 0$ ($\Delta m^2_{13} < 0$) case. Then, the CP trajectories winds to the opposite directions with those at $E = 0.5\,\mathrm{GeV}$.

4. Principle of choosing beam energies for long-baseline neutrino oscillation experiments

The intriguing features of the CP trajectory diagram mentioned above implies a new principle for determining neutrino beam energies for given oscillation parameters and the baseline length.

To avoid a confusion in notations that might occur when a major and a minor axes switch with each other depending upon the parameters we use in this section

JHEP10(2001)001

the terms the "radial thickness" and the "polar thickness" of contours. In figure 1*a*–*c* (figure 1*d*), the polar thickness denotes the length of major (minor) axis, while the radial thickness implies that of minor (major) axis.

As explained in the last section, the radial and the polar thickness of the CP trajectory diagram are the measure for $\cos\delta$ and $\sin\delta$ terms in the oscillation probability, respectively. Now we try to maximize these thickness by tuning experimental parameters for a given set of mixing parameters. It is of course important to have a large $\sin\delta$ term because it is the signal for genuine CP violation. On the other hand, to maximize the radial thickness is to help in resolving the problem of two-fold ambiguity which was discussed in the last two sections. We believe that the latter is important in view of uncertainties due to statistical and systematic errors which would inevitably exist in any experiments. If we make a choice of, for example, $E = 750\,\mathrm{MeV}$ for $L = 300\,\mathrm{km}$, then the contour shrinks to be approximately one-dimensional (see figure 6*b*) and there is no way to resolve the two-fold ambiguity.[2]

We note that in eq. (2.3) the coefficients of the $\cos\delta$ and the $\sin\delta$ terms are proportional to $x\sin x$ and $x\sin^2(x/2)$, respectively, where $x = \Delta m^2_{13}L/2E$. Therefore, a maximum of polar thickness, i.e., a maximum of absolute value of $\sin\delta$ term, occurs at half value of E/L of the corresponding maximum of radial thickness, coefficient of the $\cos\delta$ term. Namely, maximization of these terms implies:

$$\begin{aligned}\left(\frac{E}{1\,\mathrm{GeV}}\right)_{\cos\delta} &= 1.13, 0.47, 0.29\left(\frac{L}{300\ \mathrm{km}}\right)\left(\frac{\Delta m^2_{13}}{3\times10^{-3}\,\mathrm{eV}^2}\right),\\ \left(\frac{E}{1\,\mathrm{GeV}}\right)_{\sin\delta} &= 0.62, 0.24, 0.14\left(\frac{L}{300\ \mathrm{km}}\right)\left(\frac{\Delta m^2_{13}}{3\times10^{-3}\,\mathrm{eV}^2}\right)\end{aligned} \tag{4.1}$$

Thus, maxima of polar thickness occurs at relatively low energies, $(E)_{\sin\delta} = 620\,\mathrm{MeV}$ at $L = 295\,\mathrm{km}$ and $(E)_{\sin\delta} = 1.5\,\mathrm{GeV}$ at $L = 730\,\mathrm{km}$, in agreement with the conventional wisdom that CP violation effects are maximal at low energies. We, however, also emphasize that extremization of $\cos\delta$ term requires about twice larger values of beam energy for a fixed baseline distance. It is one of the reasons why we were led to the examination of a little bit of higher energies compared with that in ref. [16], $E = 0.5$-$2.0\,\mathrm{GeV}$ region, in this paper. The energies chosen in figure 1 turned out to be in the "right range" in compromising the requirements of maximizing the polar and the radial thicknesses of the CP trajectories.

The readers might wonder the possibility that large errors due to statistical and systematic uncertainties completely invalidate our principle of optimization of beam energies. We will demonstrate in section 6 that it does not occur at least for certain range of reasonable oscillation and experimental parameters.

[2]It would be very interesting to re-examine the problem of how to optimize the experimental parameters with use of informaton of neutrino energy obtained by reconstrucion of events in an event-by-event basis, as pointed out by A. Konaka through private communications.

JHEP10(2001)001

5. Resolving two-fold ambiguity in determination of δ

We have shown in the previous sections that there exists a two-fold ambiguity in determination of CP violating phase δ due to our ignorance of the sign of Δm^2_{13}. We discuss in this section the problem of how to resolve the ambiguity.

5.1 Chance for simultaneous measurement of δ and the sign of Δm^2_{13} in situ

Our foregoing analyses of the two-fold ambiguity have revealed the intriguing possibility that, if we are lucky, an in situ simultaneous determination of δ and the sign of Δm^2_{13} may be possible even at relatively short baseline as $L = 300\,\mathrm{km}$. Namely, the earth matter effect is comfortably large to split the two trajectories corresponding to positive and negative Δm^2_{13} such that both quantities can be measured simultaneously in a certain range of δ. Namely, if the angle δ is in the third or the fourth quadrants for positive Δm^2_{13} (the normal mass hierarchy), or if δ is in the first or the second quadrants for negative Δm^2_{13} (the inverted mass hierarchy), then measurement of $P(\nu_\mu \to \nu_e)$ and $P(\bar{\nu}_\mu \to \bar{\nu}_e)$ in neutrino and antineutrino experiments can determine both quantities simultaneously.

The statement just made above is a conservative one and the range of lucky determination of δ without ambiguity may extend to wider region, as one notices in figure 1. However, how wide is the region depends upon the mixing parameters as well as experimental uncertainties. We describe an attempt toward quantifying it in section 6 by computing numbers of events.

Our above observation sharply contrasts with the conventional belief that very long baseline as $\gtrsim 1,000\,\mathrm{km}$ is required for the determination of the sign of Δm^2_{13}, and open the door to a simultaneous measurement of δ and the sign of Δm^2_{13} in situ at relatively short ($\sim 300\,\mathrm{km}$ or so) baseline.

We will further pursue the possibility of simultaneous measurement of δ and the sign of Δm^2_{13} in a single experiment which is valid for full range of δ by considering longer baseline in section 6.

5.2 Two-detector method

However, nature may not be so kind. Namely, if the true value of δ is within the experimental uncertainties to one of the two crossing points of the two trajectories, we have a two-fold ambiguity in the determination of δ. In the worst case in which δ is really close to the crossing points, one cannot resolve the two-fold ambiguity no matter how accurate were the measurement.

Then, the question is how to resolve the two-fold ambiguity. In this subsection, we discuss the two-detector method in order to resolve the two-fold ambiguity in determination of the CP violating angle δ, in case it remains in single-detector ex-

JHEP10(2001)001

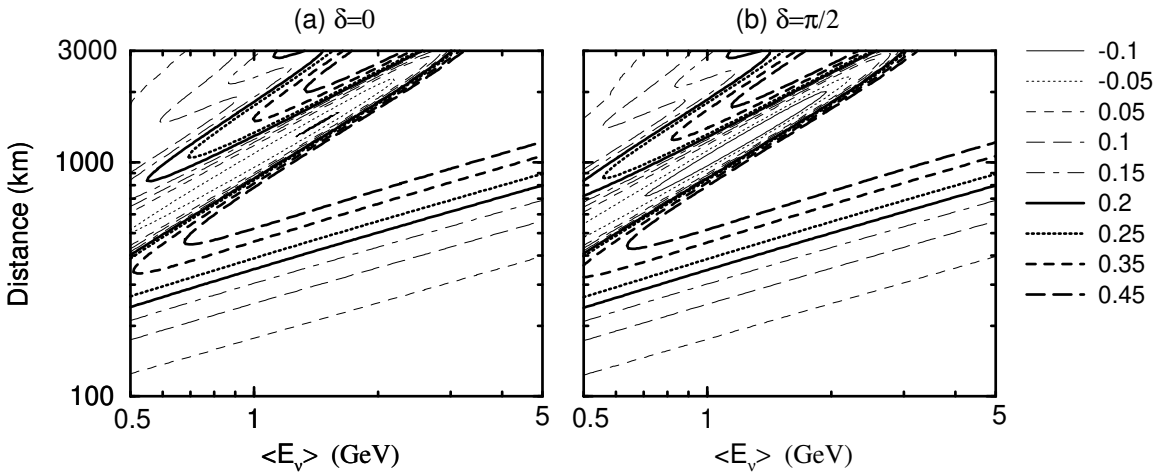

Figure 3: Asymmetry of the probability ratio defined in eq. (5.2) in the text for (a) $\delta = 0$ and (b) $\delta = \pi/2$. The mixing parameters are chosen as the same with those of figure 1.

periments. The multiple detector method has been proposed by various authors for different physical motivations [33].

We first illuminate that the two-detector option is naturally motivated by the nature of the phenomenon of neutrino oscillation itself. Let us first define the ratio of the suitably energy averaged appearance probabilities for neutrino and anti-neutrino, $R(P)$, as follows,

$$R(P) \equiv \frac{\langle P(\nu_\mu \to \nu_e)\rangle}{\langle P(\bar{\nu}_\mu \to \bar{\nu}_e)\rangle}\,. \tag{5.1}$$

We note that if there is no CP violating phase and matter effect, $R(P)$ does neither depend on the baseline nor on the average neutrino energy as long as energy distributions of neutrino and anti-neutrino are the same. Some dependence of $R(P)$ on the baseline can indicate either genuine CP violating effect or matter effect, or both. However, by simply looking at $R(P)$, it may be difficult to separate these two effects.

In order to see for which energy and baseline the matter effect could be important, independent of the magnitude of CP phase, let us define the asymmetry of the ratio $R(P)$ as follows,

$$A(R) \equiv \frac{R(P;\Delta m^2_{13} > 0) - R(P;\Delta m^2_{13} < 0)}{R(P;\Delta m^2_{13} > 0) + R(P;\Delta m^2_{13} < 0)}\,. \tag{5.2}$$

A large value of the asymmetry implies that the matter effect is enhanced relative to the vacuum effect. In fact, if there is no matter effect, from the expression of vacuum probability (2.3), this quantity is expected to be small for any values of δ.

In figure 3 plotted is the asymmetry $A(R)$ for two typical values of CP violating angle, $\delta = 0$ and $\delta = \pi/2$. The mixing parameters are chosen as the same with those of figure 1. There are several characteristic features in the figures. First of all, as

JHEP10(2001)001

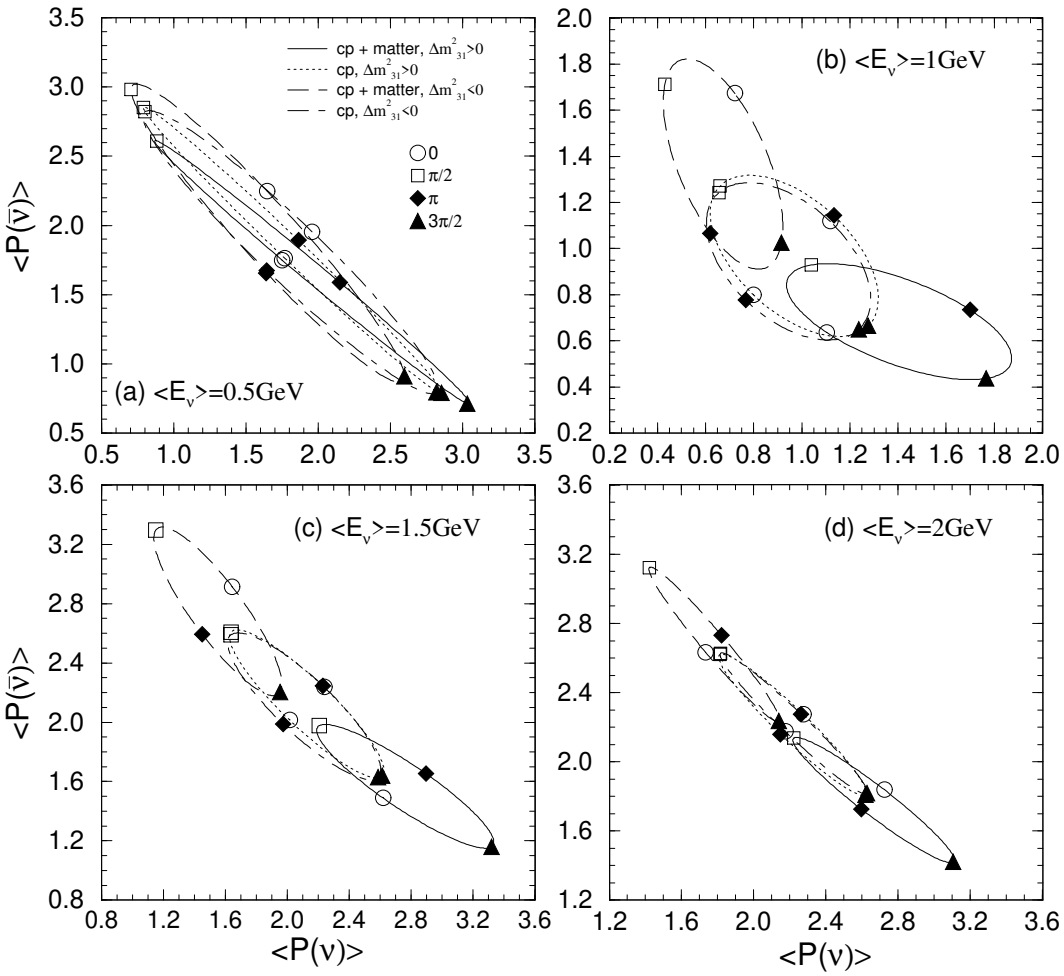

Figure 4: The same as in figure 2 but for $L = 700\,\text{km}$.

expected, the asymmetry depends very weakly on δ. The asymmetry tends to be positive, indicating that $\Delta m^2_{13} > 0$ case is enhanced compared to $\Delta m^2_{13} < 0$ case. There are two distinct regions in which the asymmetry $A(R)$ is large and positive. At $E \sim 1\,\text{GeV}$, they are at $L \sim 600 - 700\,\text{km}$, and at $1000 - 1500\,\text{km}$.

We have repeated the similar computation to obtain the CP trajectory diagram for the path lengths $L = 700$ and $1000\,\text{km}$, and energies $E = 0.5$, 1.0, 1.5, and $2\,\text{GeV}$. The results are presented in figures 4 and 5. By looking into figures 1, 4 and 5, we immediately observe several distinct features:

1. There are cases with longer baselines in which the neutrino and the antineutrino trajectory do not intersect; $E = 1.0, 1.5, 2.0\,\text{GeV}$ at $L = 700\,\text{km}$, and $E = 1.5, 2.0\,\text{GeV}$ at $L = 1000\,\text{km}$. We note that this is consistent with what we presented in figure 3 where we can see that these values of experimental parameter fall in the region of strong asymmetry defined in eq. (5.2). It resolves the two-fold degeneracy we talked about. Of course, by focusing these experimental parameters, one can determine δ and the sign of Δm^2_{13} simultane-

JHEP10(2001)001

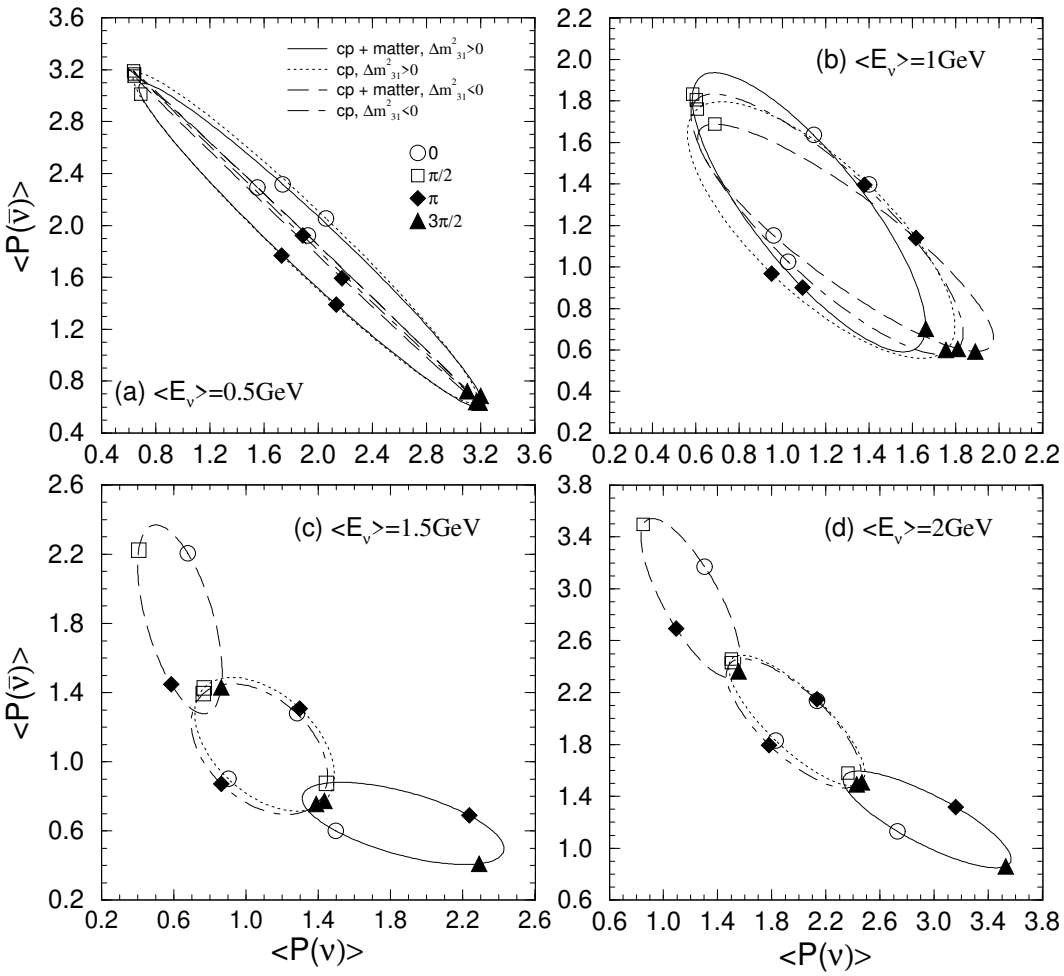

Figure 5: The same as in figure 2 but for $L = 1000\,\mathrm{km}$.

ously, provided that statistical and systematic uncertainties are small enough. It raises an important possibility that simultaneous determination of δ and the sign of Δm^2_{13} can be done in full range of δ with optimal distance of $L \simeq 700\,\mathrm{km}$. We will further discuss the possibility including experimental uncertainties in the next section.

2. The path-length dependence of the trajectory diagram is not always smooth. For example, the feature displayed in $E = 1\,\mathrm{GeV}$ at $L = 1000\,\mathrm{km}$ case does not fall into a smooth extrapolation of the behavior of $L = 295$ and $700\,\mathrm{km}$ at the same energy.

3. Some curious behavior is observed in the cases, $E = 0.5\,\mathrm{GeV}$ at $L = 700$ and $1000\,\mathrm{km}$, where the matter probabilities have similar behavior with those of vacuum oscillation, which seems to be also consistent with the results in

JHEP10(2001)001

figure 3. Most probably, it is a new phenomena, not a remnant of the vacuum mimicking phenomenon, whose interpretation is not known at the moment.

A tentative conclusion before examining the numbers of events is that by using the second detector placed at distances of 700 km or 1000 km, the two-fold ambiguity will be resolved if it remains in shorter baseline JHF-type experiments.

6. Long-baseline neutrino oscillation experiments with superbeams; some concrete examples

In discussions in the foregoing sections we have concentrated on illuminating global structure of the neutrino oscillations in the region relevant for low energy experiments, and did not pay enough attention to the statistical and the systematic uncertainties. Of course, they are of key importance in judging what is the optimal design of the experiments. On the other hand, it is not quite possible to determine at this moment which is the optimal design because we do not know the value of key parameters, most importantly θ_{13}. Therefore, our discussion in this paper is inevitably restricted to the one that may be called, at best, case studies.

In this section we first try to estimate the numbers of events including signal and the background by taking the same typical mixing parameters as the one we used before, which correspond to the LMA solution of the solar neutrino problem. We do this by taking the concrete examples of upgraded long-baseline neutrino oscillation experiment which utilizes a conventional neutrino superbeam. For definiteness, we assume a 4 MW proton beam which is planned to be constructed in the Phase II of the JHF project, and consider 1 Mton Super-Kamiokande type water Cherenkov detector whose fiducial volume is assumed to be 0.9 Mton. Such detector is already discussed by the Super-Kamiokande group who mainly motivated by an extensive search for proton decay under the name of Hyper-Kamiokande project [34]. The goal of our study in the present section is not to develop the experimental proposal which is ready to submit, but to obtain a feeling on what are the promising possibilities which deserve further detailed studies, possibly by joint collaboration by theorists and experimentalists.

We discuss three options,

(i) Single detector at $L = 300$ km.

(ii) Single detector at $L = 700/1000$ km.

(iii) Two detectors at $L = 300$ and $700/1000$ km.

In this work, we will use two types of different neutrino beams with quasi-monochromatic energy spectrum calculated by the JHF-SK Neutrino Working Group

JHEP10(2001)001

[25], which are (i) narrow band (NB) beam and (ii) off axis (OA) beam. NB beam is made by pions with particular choice of momentum selected by dipole magnet placed between two horns in the wide band beam configuration. We use in our analysis two different options of NB beam characterized by pion momenta of 2 and 3 GeV, which peaks at $\sim 1\,\mathrm{GeV}$ and $1.4\,\mathrm{GeV}$, respectively. OA beam is an another way of making quasi-monochromatic neutrino beam proposed in Beavis et al. in [33]. It is obtained by slightly (a few degrees) displaced the direction of axis of wide band beam from the far detector direction. For this type of beam, we use the ones obtained with off axis of 3 and 2 degrees, which peaks at $\sim 0.5\,\mathrm{GeV}$ and $0.8\,\mathrm{GeV}$, respectively. While we adopt as the basic parameters the ones calculated for the JHF neutrino experiment, we do hope that the results of our calculation are illuminative enough for future projects on other continents as well.

6.1 Method for calculation of number of events

Before proceeding to physics discussions we have to explain first how we calculate expected numbers of events. In our computation, we take into account both signal and background, which are calculated by the way as explained below.

Signal consists of the contributions from charged current (CC) ν_e (coming from $\nu_\mu \to \nu_e$ oscillation) interactions, which are classified into quasi-elastic (qe); $\nu + N \to \ell + N'$, one pion production (1π); $\nu + N \to \ell + N' + \pi$, multi pion production ($\mathrm{m}\pi$); $\nu + N \to \ell + N' + n\pi$, and coherent pion ($\mathrm{c}\pi$) production; $\nu + {}^{16}\mathrm{O} \to \nu + {}^{16}\mathrm{O} + \pi^+$, reactions. In our computation, we define the signal coming from the CC interactions in the expected number of events, N_{sig}, as follows,

$$N_{\mathrm{sig}} \equiv T \sum_{i=qe,1\pi,m\pi,c\pi} N_T^i \int dE \sigma^i{}_{CC}(E) \phi^0_{\nu_\mu}(E) P_{\mu e}(E) \epsilon(E)\,, \tag{6.1}$$

where N_T^i and $\sigma^i{}_{CC}(E)$ are the number of target and the CC cross section, respectively, for i-th reaction process, T is the exposure time, $\phi^0_{\nu_\mu}(E)$ is ν_μ neutrino flux at the detector site in the absence of oscillation as a function of neutrino energy, $P_{\mu e}(E)$ is the $\nu_\mu \to \nu_e$ oscillation probability, and $\epsilon(E)$ is the detection efficiency for the e-like events, which was taken from ref. [26]. See refs. [35], for the neutrino cross sections we used in this work.

We also take into account possible background which are coming from π^0 produced in the NC and the CC interactions, e/μ misidentification, and ν_e contamination in the original ν_μ beam, where the dominant ones come from π^0 produced in NC reactions as well as ν_e contamination. Following ref. [27], we express background event as

$$N_{BG} = N_{BG}^{CC} + N_{BG}^{NC} + N_{BG}^{\mathrm{beam}}\,, \tag{6.2}$$

where N_{BG}^{CC}, N_{BG}^{NC} and N_{BG}^{beam} are backgrounds coming from the CC, the NC interactions and the ν_e contamination, respectively. We compute N_{BG}^{CC} in a similar way

JHEP10(2001)001

as $N_{\rm sig}$ in eq. (6.1) but $P_{\mu e}(E)$ replaced by $P_{\mu\mu}(E)$ and $\epsilon(E)$ replaced by a constant reduction efficiency ~ 0.017 %, estimated from table 2 in ref. [27], as an approximation.

Similar to the CC interactions, contributions from NC ones include the following reactions: elastic (es); $\nu+N \to \nu+N$, one pion production; $\nu+N \to \nu+N'+\pi$, multi pion production; $\nu + N \to \nu + N' + n\pi$, and coherent pion production; $\nu +^{16}{\rm O} \to \nu +^{16}{\rm O} + \pi^0$. We can express N_{BG}^{NC} as

$$N_{BG}^{NC} \equiv \eta T \sum_{i=es,1\pi,m\pi,c\pi} N_T^i \int dE \sigma^i{}_{NC}(E) \phi^0_{\nu_\mu}(E)\,, \tag{6.3}$$

where η is the reduction efficiency, approximated as constant, which is about 0.22 % of the total NC events, estimated from table 2 in ref. [27].

The contribution from the beam ν_e contamination can be estimated in a similar way as in eqs. (6.1) and (6.3) but $\phi^0_{\nu_\mu}(E)$ replaced by $\phi^0_{\nu_e}(E)$, the ν_e flux which exists in the ν_μ flux in the absence of oscillation and $P_{\mu e}(E)$ by $P_{ee}(E)$ in eq. (6.1).

We define the expected number of "e-like" events in $\nu_\mu \to \nu_e$ channel as the sum of signal and background as,

$$N(e^-) \equiv N_{\rm sig} + N_{BG}\,. \tag{6.4}$$

For anti-neutrino channel, $\bar\nu_\mu \to \bar\nu_e$, we compute the expected number of e^+-like events in the same way properly replacing neutrino flux as well as cross sections by that of anti-neutrino.

In table 1 we present expected number of events without (which means to set $\epsilon = \eta$ =100 % in eqs.(6.1) and (6.3)) and with detection efficiency for JHF neutrino OA 2 degree beam with baseline 295 km and 0.77 MW beam power assuming Super-Kamiokande detector (22.5 kton), corresponding to the first phase configuration of the JHF neutrino project [27], with exposure of 5 years. For comparison we also present the numbers found in new JHF LOI [27]. The numbers we obtained are rather similar to those computed by the JHF working group, allowing us to have confidence that our computations are accurate enough for our purpose.

6.2 Single detector at $L = 300$ km

This is essentially identical with the upgraded JHF neutrino experiment in its Phase II. While its detailed study is underway in the working group, we try to make some suggestions here which might add (we hope) their final proposal some useful ingredients.

In order to have some feelings about the expected number of events for various JHF neutrino beam options, we show in table 2 the numbers of electron appearance events assuming 100 % $\nu_\mu \to \nu_e$ conversion, for 1 megaton SK type detector (with fiducial volume of 0.9 Mton) with baseline $L = 295$ km, and 4 MW beam power as

JHEP10(2001)001

	ν_μ CC	ν_μ NC	Beam ν_e	Oscillated ν_e
This work (before reduction)	10707	3840	270	297
This work (after reduction)	1.8	8.8	10.3	142.7
JHF Phase I (before reduction)	10714	4080	292	302
JHF Phase I (after reduction)	1.8	9.3	11.1	123.2

Table 1: Comparison of our expected number of events with that of the JHF working group for OA 2 degree beam option [27] with baseline 295 km, 0.77 MW beam power and the exposure of 5 years assuming the SK detector (22.5 kton). For the calculation of oscillated ν_e signal, $\Delta m^2_{13} = 3 \times 10^{-3}$ eV^2, $\sin^2 2\theta_{23} = 1.0$, $\sin^2 2\theta_{13} = 0.1$, and other mixing parameters are set to be zero ($\Delta m^2_{12} \to 0$, $\sin^2 2\theta_{12} \to 0$) and matter effect was neglected. For each case, upper and lower number indicate the expected number of events before reduction (or with 100 % detection efficiency) and after reduction (with reduction and/or detection efficiency).

	Narrow Band Beam		Off Axis Beam	
	2 GeV	3 GeV	3 deg.	2 deg.
Peak Energy (GeV)	~ 1.0	~ 1.4	~ 0.55	~ 0.75
ν (signal)	1.8×10^5	2.7×10^5	1.6×10^5	4.3×10^5
ν (background)	1.7×10^2	2.5×10^2	3.5×10^2	8.2×10^2
$\bar{\nu}$ (signal)	6.3×10^4	1.2×10^5	4.6×10^4	1.4×10^5
$\bar{\nu}$ (background)	0.6×10^2	1.2×10^2	1.1×10^2	2.7×10^2

Table 2: Expected numbers of e^- and e^+-like events in neutrino and anti-neutrino channels for some possible JHF neutrino beam options we use in our work, assuming 100 % conversion of $\nu_\mu \to \nu_e$ and $\bar{\nu}_\mu \to \bar{\nu}_e$, respectively. We take a 1 megaton SK-type water Cherenkov detector (assuming fiducial volume of 0.9 Mton) with baseline distance of 295 km, 4 MW beam power (corresponding to the Phase II of JHF neutrino project), and exposure of 1 year. Signal as well as background events are presented separately in the table.

planned in the Phase II of the JHF neutrino experiment with an exposure of 1 year. We also show the background which is essentially constant and does not depend on neutrino oscillation. One can estimate the expected number of events in the presence of neutrino oscillation from the numbers in the table by simply multiplying oscillation probability which is properly averaged over the cross section, neutrino energy spectrum, detection efficiency, etc.

As we emphasized at the beginning of this section the statistics heavily depends on the value of θ_{13}, on which we have no clue at present apart from the CHOOZ constraint [10]. Hence, it is difficult to judge if the experiment that we are discussing is feasible or not at this moment. Therefore, we restrict ourselves in this paper to a particular value of θ_{13}, $\sin^2 2\theta_{13} = 0.05$, which is about a half of the CHOOZ bound.

JHEP10(2001)001

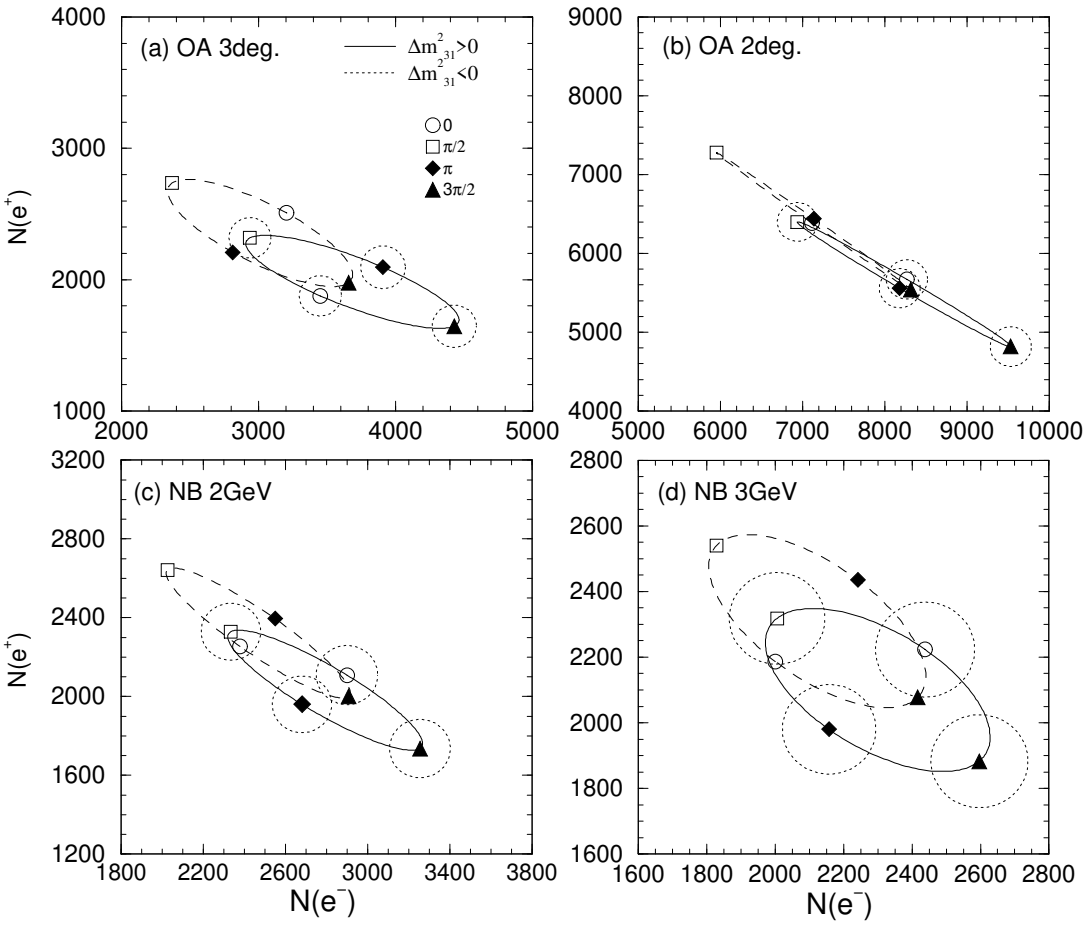

Figure 6: CP trajectory in the $N(e^-) - N(e^+)$ plane for off axis and narrow band beam for $L = 295\,\mathrm{km}$. Dotted circles indicate 3 σ errors (only statistical ones).

Now we present in figure 6 the CP trajectory contour written on the plane spanned by numbers of events (not the probabilities), $N(e^-)$ and $N(e^+)$, including the background assuming 2 and 6 years running for neutrino and anti-neutrino channels, respectively. The figure 6*a* is for OA 3 degree beam which peaks at $E \sim 0.5\,\mathrm{GeV}$, while figure 6*b* is for OA 2 degree beam which peaks at $E \sim 0.8\,\mathrm{GeV}$. figure 6*c* and 6*d* are for NB 2 and 3 GeV beams, whose energy spectra peaks at $\sim 1\,\mathrm{GeV}$ and $1.4\,\mathrm{GeV}$, respectively. We note that only for NB 3 GeV beam, we assume, as an approximation, anti-neutrino flux is the same as that of neutrino since the flux for anti-neutrino was not available for this particular beam option [25]. Dotted circles in figure 6 indicate uncertainty which corresponds to 3 σ, where only the statistical error is taken into account. Unfortunately, we have no way of estimating expected systematic errors in the super-JHF experiments.

As we noticed in section 3 there is an inversion phenomenon in the diagram. Namely, for a given shape of the contour, the low probability branch ($\cos\delta > 0$ region) in figure 6*a* is mapped into the high probability branch ($\cos\delta < 0$ region) in figure 6*b* in $\Delta m^2_{13} > 0$ case, and vice versa in $\Delta m^2_{13} < 0$ case.

JHEP10(2001)001

We point out that the feature can be used as a method of identifying the value of δ, if otherwise ambiguous in its measurement. Suppose that they run first at $E = 1\,\mathrm{GeV}$ and obtained the result which tends to prefer the high probability branch, but they were not confident because the high and the low probability branches are not so well separated. While they can just continue to run to increase statistics with the same energy in such circumstance, an alternative way (and better way, we believe) is to run at lower energies, $E \sim 0.5\,\mathrm{GeV}$. If the parameter is really in the high (low) probability branch at $E \sim 1.0\,\mathrm{GeV}$, then it must jump down (up) to the low (high) probability branch at $E \sim 0.5\,\mathrm{GeV}$.

Let us consider, for example, the case of positive Δm^2_{13}. If $\delta \simeq \pi/4$ (high probability branch), the jump is from $P(\nu) \simeq 2.05$ % at 1 GeV to $P(\nu) \simeq 1.3$ % at 0.5 GeV, as one can see in figure 1. On the other hand, if $\delta \simeq 3\pi/4$ (low probability branch) the jump is from $P(\nu) \simeq 1.85\%$ at 1 GeV to $P(\nu) \simeq 1.65$ % at 0.5 GeV. Thus, a greater downward jump of about 37 % is predicted in the case of $\delta \simeq \pi/4$, as compared to a modest ~ 10 % decrease in the $\delta \simeq 3\pi/4$ case. Thus, running at high and low energies would greatly help to distinguish the high and the low probability branches, or $\cos\delta > 0$ and $\cos\delta < 0$ cases, if the energies are tuned to have a large radial thickness. Unfortunately, we cannot resolve the two-fold ambiguity by using this technique, because the high probability branch jumps to low probability branch, or vice versa, both in $\Delta m^2_{13} > 0$ and $\Delta m^2_{13} < 0$ cases simultaneously.

It should be emphasized that, if we are lucky, we will be able to determine the CP violating angle δ and the sign of Δm^2_{13} simultaneously. It is the case with highest statistics among the cases considered in this paper, and hence it is likely to have resolving power of the both quantities. By luckiness, we mean very roughly that if the angle δ is in the third or the fourth quadrants in the case of normal mass hierarchy ($\Delta m^2_{13} > 0$), and is the first or the second quadrants in the case of inverted mass hierarchy ($\Delta m^2_{13} < 0$), respectively. In this case, the experiment will reveal by high statistics data taking the CP violating angle and the sign of Δm^2_{13} simultaneously. The accuracy of the measurement of δ would be somewhere in 20-30 degrees, if the systematic errors are not too sizable.

6.3 Single detector at $L = 700/1000\,\mathrm{km}$

We next consider the option of single detector at $L = 700/1000$ km. As we saw in section 3 the detector at $L = 700/1000$ km shows a qualitatively different characteristics; the neutrino and the antineutrino trajectory becomes nonoverlapping for neutrino energies of $1 - 2\,\mathrm{GeV}$, allowing simultaneous determination of δ and the sign of Δm^2_{13} for any values of δ, if the statistics is high enough.

In figure 7 we present the CP trajectory contours written on the $N(e^-) - N(e^+)$ plane with path length of (a, b) 500 km and (c, d) 700 km. The former is for comparison, in particular to represent the correlation between the matter effect and the

JHEP10(2001)001

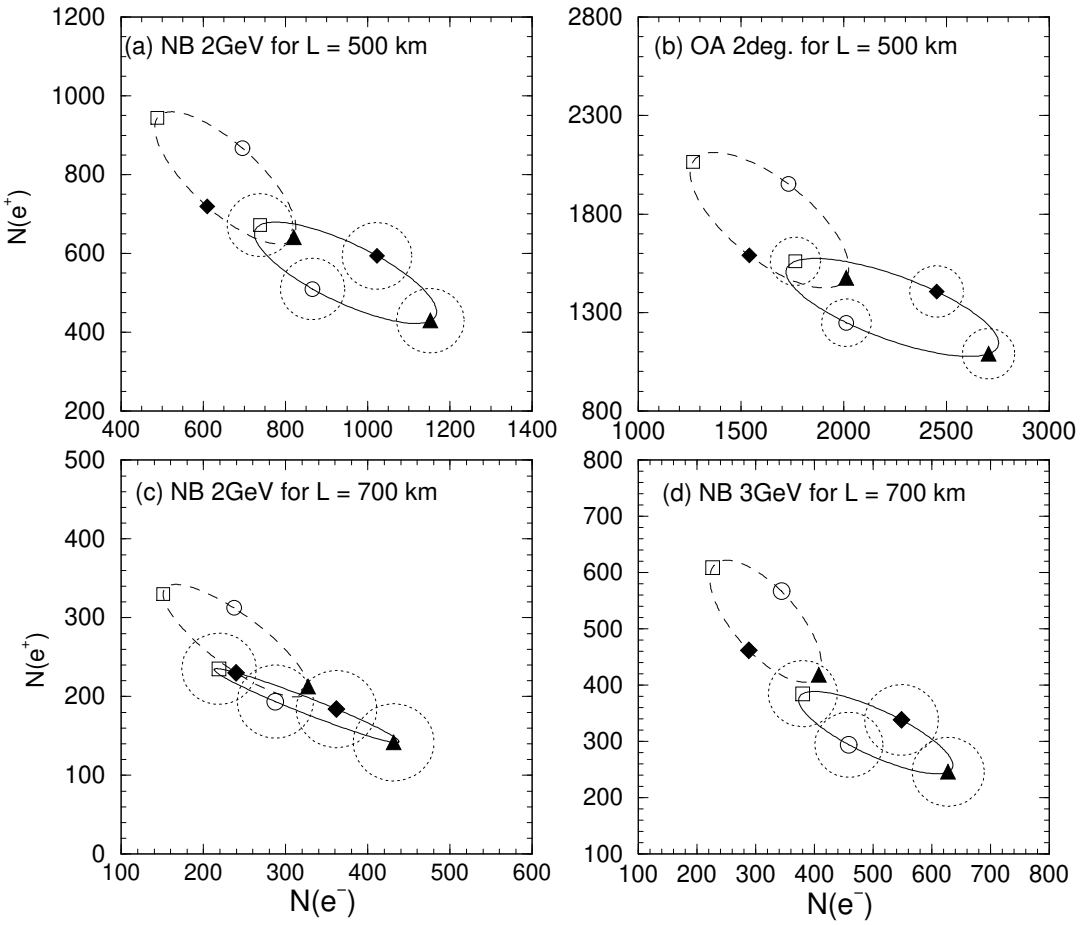

Figure 7: CP trajectory in the $N(e^-) - N(e^+)$ plane for off axis and narrow band beam for $L = 500\,\mathrm{km}$ or $700\,\mathrm{km}$. Dotted circles indicate 3 σ errors (only statistical ones). Mixing parameters are fixed to be the same as in figure 1.

number of events as a function of baseline length. Since there is no version of off-axis beam with peak energies of $\gtrsim 1\,\mathrm{GeV}$ available to us, we use NB 3 GeV beam which peaks at around $E = 1.4\,\mathrm{GeV}$. It appears that off-axis beams are more intense than narrow-band beams with similar peak energies by a factor of 2-3. If we are able to design OA beam with peak energy of $\gtrsim 1.4\,\mathrm{GeV}$, we would gain a factor of 3 in number of events. If it is the case, we may scale the abscissa and the ordinate by factor of 3 and the radii of the error circle are reduced by factor of $\sqrt{3}$. Of course, to have off-axis beam with peak energies of $\gtrsim 1\,\mathrm{GeV}$ one should probably start with a completely different proton beam design with higher energies, whose discussion is far beyond the scope of this paper.

We note that for NB 3 GeV the number of events is ~ 500 for 2 (6) years of running in neutrino (antineutrino) channel at $L = 700\,\mathrm{km}$, and ~ 2000 for $L = 500\,\mathrm{km}$. They are certainly not enormous but are not too small either. If the beam normalization is properly known it would be possible to discover the existence of leptonic CP violation and at the same time to determine the sign of Δm^2_{13}.

JHEP10(2001)001

Clearly, the conclusion depends on many unknown factors, the values of mixing parameters, θ_{13}, Δm^2_{12}, and δ and also one experimental conditions, uncertainties in absolute flux normalization, cross sections, and efficiency background rejection.

6.4 Two detectors at $L = 300$ and $700/1000$ km

Suppose that we have a bad luck in the experiment with $L = 300$ km by having δ in the alternative regions from that we have mentioned in Subsec. 6.2. Namely, if $\sin\delta > 0$ in the case of normal mass hierarchy and $\sin\delta < 0$ in the case of inverted mass hierarchy, we will be able to determine (assuming enough statistics) δ but only with modulo two-fold ambiguity. While it is already a great achievement, it may be better if we have a way to resolve the ambiguity. Motivated by the consideration in the preceding section, it is natural to consider the two-detector option, one at $L = 300$ km and the other at $L = 700/1000$ km. While it is indeed an "expensive option" which uses the two megaton detectors (or possibly one 1 Mton and one $\sim$ 100 kton iron calorimeter) it might not be an unrealistic one in view of the proposal of detectors either in Korea [36], or in Beijin [37].

In this two-detector option, the requirement of statistics can be relaxed because the second detector is effectively only for the determination of the sign of Δm^2_{13}. In view of figure 7 a narrow band beam with energy a bit higher than NB 3 GeV beam may be able to do the job, without multiplying 3 in flux normalization

7. CP trajectory diagram for neutrino factories

Finally, we briefly address in this section the features of CP trajectory diagram for physical parameters which are appropriate for neutrino factories. It is to illustrate enormous difference in the features of the CP phase-matter interplay between the situations of neutrino factory and the low energy superbeam. We neither intend to make full comparison of these two different strategies nor try to argue which is the better way to measure CP violation.

In figure 8, presented is the CP trajectory diagram for $L = 3000$ km for varying neutrino energies from 10 GeV to 50 GeV. Only the trajectories with matter effect are plotted for both sign of Δm^2_{13}. The matter density is taken as $\rho Y_e = 2$ g/cm^3 corresponding to upper mantle region. Unlike diagrams for low energy beams presented in the preceding sections the two trajectories corresponding to positive and negative Δm^2_{13} are far apart with each other. It leads to the well known fact that the matter effect dominates over the CP violating effect due to the Kobayashi-Maskawa phase.

The good news is that in the neutrino factory situation there is of course no such ambiguity as the one we discussed in this paper. (However, there arises an another ambiguity in this case, if the value of θ_{13} is not known, as pointed out by Burguet-Castell et al. [30], as mentioned in [33].) On the other hand, the problem of matter

JHEP10(2001)001

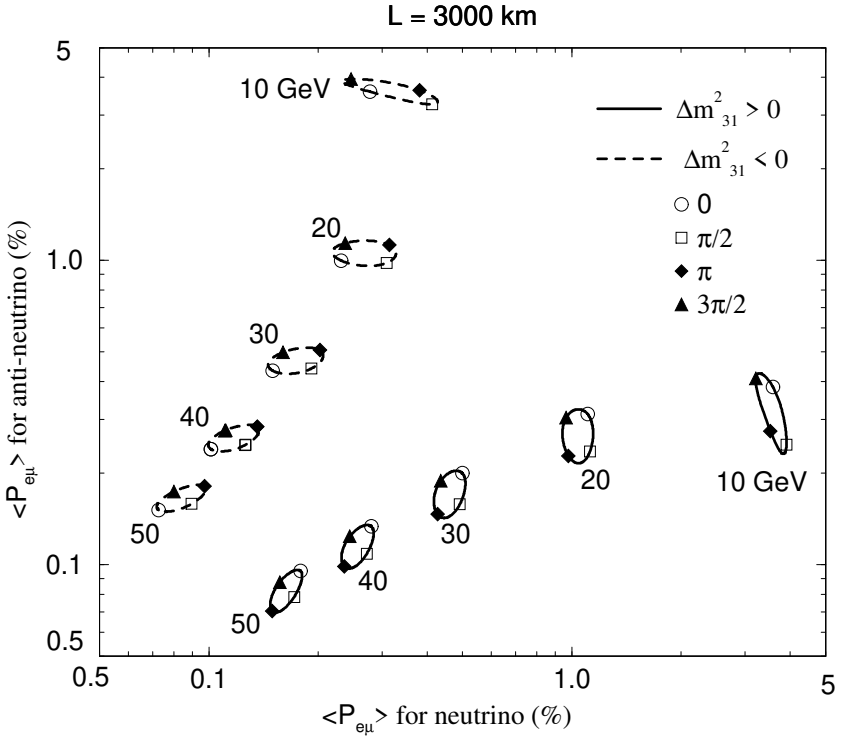

Figure 8: The CP trajectory diagram in bi-probability plane for $L = 3000\,\mathrm{km}$ and much higher neutrino energies $E = 10-50\,\mathrm{GeV}$ which correspond to so called "Neutrino Factory" situation. The mixing parameters are fixed to be the same as in figure 1 except that we take $\rho Y_e = 2.0\ \mathrm{g/cm^3}$.

effect contamination is severer. It appears to us that we need further studies to clearly separate genuine CP violating effect from the matter effect in neutrino factories.

8. Conclusion

We have discussed the features of the neutrino oscillations which are relevant for the experiments with conventional low energy (typically $\sim 1\,\mathrm{GeV}$) superbeams with mediumly-long baseline ($\lesssim 1000\,\mathrm{km}$) which aim at measuring leptonic CP violation. We have assumed, for the purpose of estimating number of events and statistical uncertainties, a supermassive 1 megaton water Cherenkov detector of Super-Kamiokande type, and 4 MW beam power as planned in the Phase II of the JHF neutrino experiment.

We started with focusing on the problem of interplay between genuine CP violation and the matter effect. While it is a widely discussed topics in the literature, we have uncovered an interesting new feature; the matter effect helps. Namely, the matter effect in such mediumly-long baseline experiments is comfortably large so that it helps to resolve the (approximate) two-fold ambiguity which would exist, in the absence of the effect, in the vacuum oscillation probability.

JHEP10(2001)001

To elucidate the features of the CP phase-matter interplay, we have introduced a new powerful tool called the "CP trajectory diagram in bi-probability space". The diagram allows us to represent pictorially the following three effects separately in a single diagram in a compact form: 1) the genuine CP violating effect due to the leptonic Kobayashi-Maskawa phase δ, or $\sin\delta$, the CP odd term, 2) the effect due to the CP even term, $\cos\delta$, and 3) the fake CP violating effect due to the earth matter. As discussed in the text, the effect of the CP odd term is characterized by the "polar thickness" whereas the effect of the CP even term is characterized by the "radial thickness" of the trajectory contour (see the beginning of section 4 for the definitions of "polar" and "radial" thickness). On the other hand, the earth matter effect is characterized by the distance of separation between the two trajectory contours with different sign of Δm^2_{13}.

By using such diagram, we have observed that there is a two-fold ambiguity in the determination of the CP violating angle δ, if we do not know *a priori* the sign of Δm^2_{13}. The ambiguity is shown to be a remnant of the approximate symmetry possessed by the vacuum oscillation probability (as mentioned above) under simultaneous transformation of $\delta \to \pi - \delta$ and $\Delta m^2_{13} \to -\Delta m^2_{13}$. We have discussed the principle of "maximal fatness" of the CP trajectory diagram to find optimal experimental parameters in order to have a large CP violation and at the same time to resolve such two-fold ambiguity.

By these considerations we are naturally invited to consider the possibility of measuring simultaneously the CP phase δ as well as the sign of Δm^2_{13}. We have discovered the enlightening possibility that such simultaneous measurement can be done with relatively short baseline, $L \simeq 300\,\mathrm{km}$ assuming 1 megaton water Cherenkov detector, as in the phase II of JHF-Kamioka neutrino experiment. It works, however, only under the condition of nature's kind setting of the parameter into the region $\sin\delta \cdot \Delta m^2_{13} < 0$.

We also described a way of resolving the degeneracy in the case of unresolved high and the low probability branches, or $\cos\delta > 0$ and $\cos\delta < 0$ region for $\Delta m^2_{13} > 0$ case, and vice versa in $\Delta m^2_{13} < 0$ case. By running at high ($\sim 1\,\mathrm{GeV}$) and low ($\sim 0.5\,\mathrm{GeV}$) beam energies the high and low probability branches are interchanged with each other, and this effect may help in identifying δ while it cannot resolve the two-fold ambiguity.

Furthermore, we have uncovered an interesting possibility that simultaneous measurement of δ and the sign of Δm^2_{13} can be done in situ for the whole region of δ ($0 < \delta < 2\pi$) in the experiments with longer baseline distance, $L \sim 700\,\mathrm{km}$ (corresponding to the CERN to Gran Sasso and/or Fermilab to Soudan-2 distances), again with a megaton water Cherenkov detector.

We also briefly discussed how the CP trajectory diagram look like for the neutrino factory situation and observed that the two CP trajectory with different signs of Δm^2_{13} are well separated owing to the fact that the matter effect is dominant. It

JHEP10(2001)001

is in sharp contrast with the case of low energy superbeam, the main subject of this paper. A clear way of separating the CP phase effect from the matter effect is naturally called for.

We hope that our discussions in this paper would help in designing the future neutrino oscillation experiments.

Acknowledgments

We have been greatly benefited by massive communications with members of the JHF-SK Neutrino Working Group, in particular, Akira Konaka, Takashi Kobayashi, and most intensively, Yoshihisa Obayashi for numerous valuable informative correspondences on low energy neutrino beams and detector backgrounds, and sharing with us many preliminary informations of the JHF experiments which are prepared for the new version of the Letter of Intent that appeared quite recently.

One of us (H.M.) thanks Marcelo M. Guzzo and the Department of Cosmic Ray and Chronology at Gleb Wataghin Physics Institute in UNICAMP for their hospitality during his visit where part of this work was done. This work was supported by the Brazilian funding agency Fundação de Amparo à Pesquisa do Estado de São Paulo (FAPESP), and by the Grant-in-Aid for Scientific Research in Priority Areas No. 12047222, Japan Ministry of Education, Culture, Sports, Science and Technology.

A. Proof of ellipticity of CP trajectory diagram

We give a proof that the CP trajectory is elliptic in this Appendix. It can be shown under the assumption of mass (Δm^2) hierarchy and the adiabatic approximation that the neutrino and the antineutrino oscillation probabilities can be written in the following forms:

$$\begin{aligned} P(\nu) &= A\cos\delta + B\sin\delta + C \\ P(\bar{\nu}) &= \bar{A}\cos\delta - \bar{B}\sin\delta + \bar{C} \end{aligned} \tag{A.1}$$

It is true in all the perturbative formula so far derived in refs. [20]–[23]. However, we should note that it is not true in the exact formula derived in [38]. Therefore, it is not an exact formula apart from the case in vacuum, but is a very good one in the case of hierarchical mass difference we are interested in.

Once the above general form holds for a fixed arbitrary energy, it hold even if one take average over an arbitrary neutrino energy spectrum. Therefore, we implicitly imply P's and the coefficients in (A.1) as averaged over an energy spectrum, though it is not indicated explicitly. Hence, the general form applies to the CP trajectory

JHEP10(2001)001

diagram on bi-number-of-event plane, with which we have dealt in section 6. (In fact, this general form applies even if we take average over the neutrino path length.)

By eliminating δ we obtain the equation obeyed by $P(\nu)$ and $P(\bar{\nu})$ as

$$\frac{1}{\left(\frac{A}{B}+\frac{\bar{A}}{\bar{B}}\right)^2}\left(\frac{P(\nu)-C}{B}+\frac{P(\bar{\nu})-\bar{C}}{\bar{B}}\right)^2+\frac{1}{\left(\frac{B}{A}+\frac{\bar{B}}{\bar{A}}\right)^2}\left(\frac{P(\nu)-C}{A}-\frac{P(\bar{\nu})-\bar{C}}{\bar{A}}\right)^2=1\,. \tag{A.2}$$

In vacuum, the expression simplifies because $A=\bar{A}$ etc.:

$$\left(\frac{P(\nu)+P(\bar{\nu})-2C}{2A}\right)^2+\left(\frac{P(\nu)-P(\bar{\nu})}{2B}\right)^2=1\,, \tag{A.3}$$

which implies that the minor (if $A>B$) or major (if $A<B$) axes are always at 45 degree.

This completes the proof that the CP trajectory is elliptic.

References

[1] KAMIOKANDE collaboration, Y. Fukuda et al., *Atmospheric $\nu_\mu\nu_e$ ratio in the multi-GeV energy range*, *Phys. Lett.* **B 335** (1994) 237;
SUPER-KAMIOKANDE collaboration, Y. Fukuda et al., *Evidence for oscillation of atmospheric neutrinos*, *Phys. Rev. Lett.* **81** (1998) 1562 [hep-ex/9807003]; *Tau neutrinos favored over sterile neutrinos in atmospheric muon neutrino oscillations*, *Phys. Rev. Lett.* **85** (2000) 3999 [hep-ex/0009001];
T. Kajita, *Atmospheric neutrino results from super-kamiokande and kamiokande: evidence for ν/μ oscillations*, in *Neutrino physics and astrophysics*, Proceedings of the XVIIIth International Conference on Neutrino Physics and Astrophysics (Neutrino '98), June 4-9, 1998, Takayama, Japan, Y. Suzuki and Y. Totsuka eds., Elsevier, Amsterdam 1999, p. 123 *Nucl. Phys.* **77** *(Proc. Suppl.)* (1999) 123 [hep-ex/9810001].

[2] HOMESTAKE collaboration, K. Lande et al., *Measurement of the solar electron neutrino flux with the Homestake Chlorine detector*, *Astrophys. J.* **496** (1998) 505;
SAGE collaboration, J.N. Abdurashitov et al., *Measurement of the solar neutrino capture rate with gallium metal*, *Phys. Rev.* **D 60** (1999) 055801 [astro-ph/9907113];
GALLEX collaboration, W. Hampel et al., *Gallex solar neutrino observations: results for gallex IV*, *Phys. Lett.* **B 447** (1999) 127;
KAMIOKANDE collaboration, Y. Fukuda et al., *Solar neutrino data covering solar cycle 22*, *Phys. Rev. Lett.* **77** (1996) 1683;
SUPER-KAMIOKANDE collaboration, Y. Fukuda et al., *Measurements of the solar neutrino flux from super-Kamiokande's first 300 days*, *Phys. Rev. Lett.* **81** (1998) 1158 [hep-ex/9805021], erratum *ibid.* **81** (1998) 4279; *Measurement of the solar neutrino energy spectrum using neutrino electron scattering*, *Phys. Rev. Lett.* **82** (1999) 2430 [hep-ex/9812011]; *Constraints on neutrino oscillation parameters from the measurement of day-night solar neutrino fluxes at Super-Kamiokande*, *Phys. Rev. Lett.* **82**

JHEP10(2001)001

(1999) 1810 [hep-ex/9812009];
SuperKamiokande collaboration, S. Fukuda et al., *Solar ^8B and hep neutrino measurements from 1258 days of super-kamiokande data*, *Phys. Rev. Lett.* **86** (2001) 5651 [hep-ex/0103032]; *Constraints on neutrino oscillations using 1258 days of Super-Kamiokande solar neutrino data*, *Phys. Rev. Lett.* **86** (2001) 5656 [hep-ex/0103033].

[3] SNO collaboration, Q.R. Ahmad et al., *Measurement of the charged of current interactions produced by b-8 solar neutrinos at the sudbury neutrino observatory*, *Phys. Rev. Lett.* **87** (2001) 071301 [nucl-ex/0106015];
see also http://www.sno.phy.queensu.ca/sno/first_results/.

[4] Super-Kamiokande collaboration, Y. Fukuda *et al.*, in ref. [2]

[5] K2K collaboration, S.H. Ahn et al., *Detection of accelerator produced neutrinos at a distance of 250 km*, *Phys. Lett.* **B 511** (2001) 178 [hep-ex/0103001];
see also http://neutrino.kek.jp/news/2001.07.10.News/index-e.html.

[6] Z. Maki, M. Nakagawa and S. Sakata, *Remarks on the unified model of elementary particles*, *Prog. Theor. Phys.* **28** (1962) 870.

[7] M. Kobayashi and T. Maskawa, *CP violation in the renormalizable theory of weak interaction*, *Prog. Theor. Phys.* **49** (1973) 652.

[8] The early references on leptonic CP violation include: N. Cabibbo, *Time reversal violation in neutrino oscillation*, *Phys. Lett.* **B 72** (1978) 333;
V. Barger, K. Whisnant and R.J.N. Phillips, *CP-violation in three neutrino oscillations*, *Phys. Rev. Lett.* **45** (1980) 2084;
S. Pakvasa, in *Proceedings of the XXth International Conference on High Energy Physics*, L. Durand and L. G. Pondrom eds., AIP Conf. Proc. No. 68 (AIP, New York, 1981), vol. 2, pp. 1164;
S.M. Bilenkii, J. Hosek and S.T. Petcov, *On oscillations of neutrinos with dirac and majorana masses*, *Phys. Lett.* **B 94** (1980) 495;
P.I. Krastev and S.T. Petcov, *Resonance amplification and T violation effects in three neutrino oscillations in the earth*, *Phys. Lett.* **B 205** (1988) 84;
S. Toshev, *Maximal T violation in matter*, *Phys. Lett.* **B 226** (1989) 335.

[9] H. Minakata, *The three neutrino scenario*, *Nucl. Phys.* **100** *(Proc. Suppl.)* (2001) 237 [hep-ph/0101231].

[10] CHOOZ collaboration, M. Apollonio et al., *Initial results from the chooz long baseline reactor neutrino oscillation experiment*, *Phys. Lett.* **B 420** (1998) 397 [hep-ex/9711002]; *Limits on neutrino oscillations from the CHOOZ experiment*, *Phys. Lett.* **B 466** (1999) 415;
See also, The Palo Verde Collaboration, F. Boehm et al., *Results from the palo verde neutrino oscillation experiment*, *Phys. Rev.* **D 62** (2000) 072002 [hep-ex/0003022].

JHEP10(2001)001

[11] JHF Neutrino Working Group, Y. Itow et al., *Letter of intent: a long baseline neutrino oscillation experiment using the JHF 50 GeV proton-synchrotron and the Super-Kamiokande detector*, February 3, 2000.

[12] The MINOS Collaboration, P. Adamson et al., *MINOS Detectors Technical Design Report, Version 1.0*, NuMI-L-337, October 1998

[13] OPERA Collaboration, M. Guler et al., *OPERA: an appearance experiment to search for $\nu_\mu \leftrightarrow \nu_\tau$ oscillations in the CNGS beam. Experimental proposal*, CERN-SPSC-2000-028, CERN-SPSC-P-318, LNGS-P25-00, Jul 2000.

[14] H. Minakata and H. Nunokawa, *Inverted hierarchy of neutrino masses disfavored by supernova 1987a*, *Phys. Lett.* **B 504** (2001) 301 [hep-ph/0010240].

[15] S.P. Mikheev and A.Y. Smirnov, *Resonant amplification of neutrino oscillations in matter and solar neutrino spectroscopy*, *Nuovo Cim.* **C9** (1986) 17;
L. Wolfenstein, *Neutrino oscillations in matter*, *Phys. Rev.* **D 17** (1978) 2369.

[16] H. Minakata and H. Nunokawa, *Measuring leptonic CP-violation by low energy neutrino oscillation experiments*, *Phys. Lett.* **B 495** (2000) 369 [hep-ph/0004114].

[17] H. Minakata and H. Nunokawa, *Measuring CP-violation by low-energy medium-baseline neutrino oscillation experiments*, hep-ph/0009091.

[18] B. Richter, *Conventional beams or neutrino factories: the next generation of accelerator-based neutrino experiments*, hep-ph/0008222.

[19] Some recent discussions of the vacuum mimicking mechanism may be found in [9] and in S.J. Parke and T.J. Weiler, *Optimizing T-violating effects for neutrino oscillations in matter*, *Phys. Lett.* **B 501** (2001) 106 [hep-ph/0011247];
P. Lipari, *CP-violation effects and high energy neutrinos*, *Phys. Rev.* **D 64** (2001) 033002 [hep-ph/0102046];
E.K. Akhmedov, *Matter effects in short-baseline neutrino oscillations*, *Phys. Lett.* **B 503** (2001) 133 [hep-ph/0011136];
O. Yasuda, *Vacuum mimicking phenomena in neutrino oscillations*, *Phys. Lett.* **B 516** (2001) 111 [hep-ph/0106232].

[20] J. Arafune and J. Sato, *CP and T violation test in neutrino oscillation*, *Phys. Rev.* **D 55** (1997) 1653 [hep-ph/9607437];
J. Arafune, M. Koike and J. Sato, *CP-violation and matter effect in long baseline neutrino oscillation experiments*, *Phys. Rev.* **D 56** (1997) 3093 [hep-ph/9703351], erratum *ibid.* **D60** (1997) 119905.

[21] H. Minakata and H. Nunokawa, *How to measure CP-violation in neutrino oscillation experiments?*, *Phys. Lett.* **B 413** (1997) 369 [hep-ph/9706281].

[22] H. Minakata and H. Nunokawa, *CP-violation vs. matter effect in long-baseline neutrino oscillation experiments*, *Phys. Rev.* **D 57** (1998) 4403 [hep-ph/9705208].

JHEP10(2001)001

[23] M. Tanimoto, *Is CP-violation observable in long baseline neutrino oscillation experiments?*, *Phys. Rev.* **D 55** (1997) 322 [hep-ph/9605413]; *Prediction on CP violation in long baseline neutrino oscillation experiments*, *Prog. Theor. Phys.* **97** (1997) 901 [hep-ph/9612444];
S.M. Bilenkii, C. Giunti and W. Grimus, *Long-baseline neutrino oscillation experiments and CP-violation in the lepton sector*, *Phys. Rev.* **D 58** (1998) 033001 [hep-ph/9712537];
O. Yasuda, *Three flavor neutrino oscillations and application to long baseline experiments*, *Acta Phys. Polon.* **B30** (1999) 3089;
M. Koike and J. Sato, *CP and t violation in long baseline experiments with low energy neutrino from muon storage ring*, *Phys. Rev.* **D 61** (2000) 073012 [hep-ph/9909469], erratum *ibid.* **D62** (2000) 079903;
K. Dick, M. Freund, M. Lindner and A. Romanino, *CP-violation in neutrino oscillations*, *Nucl. Phys.* **B 562** (1999) 29 [hep-ph/9903308];
T. Ota and J. Sato, *Matter profile effect in neutrino factory*, *Phys. Rev.* **D 63** (2001) 093004 [hep-ph/0011234];
T. Miura, E. Takasugi, Y. Kuno and M. Yoshimura, *The matter effect to T-violation at a neutrino factory*, *Phys. Rev.* **D 64** (2001) 013002 [hep-ph/0102111].

[24] CERN WORKING GROUP ON SUPER BEAMS collaboration, J.J. Gomez-Cadenas et al., *Physics potential of very intense conventional neutrino beams*, hep-ph/0105297.

[25] T. Kobayashi, Talk at 5th TOKUTEI-RCCN Workshop, Institute for Cosmic Ray Research, Chiba, Japan, February 23-24, 2001, and private communications.

[26] Y. Obayashi, Talk at Workshop on JHF-SK Neutrino Oscillation Experiment, April 3-4, 2001, KEK, Tsukuba, Japan and private communications.

[27] Y. Itow et al., *The JHF-Kamioka neutrino project*, hep-ex/0106019.

[28] A. De Rujula, M.B. Gavela and P. Hernandez, *Neutrino oscillation physics with a neutrino factory*, *Nucl. Phys.* **B 547** (1999) 21 [hep-ph/9811390];
A. Blondel et al., *The neutrino factory: beam and experiments*, *Nucl. Instrum. Meth.* **A451** (2000) 102;
A. Cervera, A. Donini, M.B. Gavela, J.J. Gomez Cadenas, P. Hernandez, O. Mena and S. Rigolin, *Golden measurements at a neutrino factory*, *Nucl. Phys.* **B 579** (2000) 17 [hep-ph/0002108], erratum *ibid.* **B593** (2000) 731;
A. Donini, M.B. Gavela, P. Hernandez and S. Rigolin, *Four species neutrino oscillations at ν-factory: Sensitivity and CP-violation*, *Nucl. Instrum. Meth.* **A451** (2000) 58.

[29] S. Geer, *Neutrino beams from muon strage rings characteristics and physics potential*, *Phys. Rev.* **D 57** (1998) 6989 [hep-ph/9712290], erratum *ibid.* **D59** (1999) 039903;
V. Barger, S. Geer and K. Whisnant, *Long baseline neutrino physics with a muon storage ring neutrino source*, *Phys. Rev.* **D 61** (2000) 053004 [hep-ph/9906487];

JHEP10(2001)001

V. Barger, S. Geer, R. Raja and K. Whisnant, *Long-baseline study of the leading neutrino oscillation at a neutrino factory*, *Phys. Rev.* **D 62** (2000) 013004 [hep-ph/9911524]; *Neutrino oscillations at an entry-level neutrino factory and beyond*, *Phys. Rev.* **D 62** (2000) 073002 [hep-ph/0003184]; *Short-baseline neutrino oscillations at a neutrino factory*, *Phys. Rev.* **D 63** (2001) 033002 [hep-ph/0007181];
C. Albright et al., *Physics at a neutrino factory*, hep-ex/0008064.

[30] V. Barger, S. Geer, R. Raja and K. Whisnant, *Exploring neutrino oscillations with superbeams*, *Phys. Rev.* **D 63** (2001) 113011 [hep-ph/0012017];
V. Barger et al., *Oscillation measurements with upgraded conventional neutrino beams*, hep-ph/0103052;
K. Dick, M. Freund, P. Huber and M. Lindner, *A comparison of the physics potential of future long baseline neutrino oscillation experiments*, *Nucl. Phys.* **B 598** (2001) 543 [hep-ph/0008016];
M. Koike, T. Ota and J. Sato, *Ambiguities of theoretical parameters and CP/T violation in neutrino factories*, hep-ph/0011387;
J. Burguet-Castell, M.B. Gavela, J.J. Gomez-Cadenas, P. Hernandez and O. Mena, *On the measurement of leptonic CP-violation*, *Nucl. Phys.* **B 608** (2001) 301 [hep-ph/0103258];
J. Pinney and O. Yasuda, *Correlations of errors in measurements of CP-violation at neutrino factories*, *Phys. Rev.* **D 64** (2001) 093008 [hep-ph/0105087].

[31] G.L. Fogli, E. Lisi, D. Montanino and A. Palazzo, *Three-flavor msw solutions of the solar neutrino problem*, *Phys. Rev.* **D 62** (2000) 013002 [hep-ph/9912231].

[32] Part of the results in this paper has been announced: H. Minakata, *CP trajectory diagram*, talk at The 3rd International Workshop on *Neutrino factories based on muon strage rings (NuFACT'01)*, May 24-30, 2001, Tsukuba, Japan. See, http://www-prism.kek.jp/nufact01/May29/WG1/29wg1_minakata.pdf.

[33] In the Brookhaven proposal of long baseline neutrino oscillation experiment the two-detector method is advocated to have increased sensitivity in measurement of the disappearance effect. See E889 collaboration, D. Beavis et al., *Long baseline neutrino oscillation experiment at the AGS approved by the HENPAC as AGS experiment 889. Physics design report*, BNL No. 52459, April 1995. We have discussed the two- and three-detector methods to extract the CP violating piece of the neutrino oscillation probabilities without doing antineutrino (or neutrino) experiment [21]. Very recently, Burguet-Castell et al. in [30] discussed two-detector method for resolving a similar two-fold ambiguity in the simultaneous determination of δ and θ_{13} in neutrino factory

[34] M. Shiozawa, talk at Workshop on JHF-SK Neutrino Oscillation Experiment, April 3-4, 2001, KEK, Tsukuba, Japan.

[35] K. Okumra, *Observation of atmospheric neutrinos in Super-Kamiokande and a neutrino oscillation analysis*, Doctor thesis, University of Tokyo, February, 1999;

JHEP10(2001)001

K. Ishihara, *Study of $\nu_\mu \to \nu_\tau$ and $\nu_m u \to \nu_{sterile}$ neutrino oscillations with the atmospheric neutrino data in Super-Kamiokande*, Doctor thesis, University of Tokyo, December, 1999, available from
`http://www-sk.icrr.u-tokyo.ac.jp/doc/sk/pub/index.html`.

[36] S.B. Kim, talk at KOSEF-JSPS Joint Seminar on New Developments in Neutrino Physics, October 16-20, 2000, Seoul Korea, published in Proceedings, p. 182.

[37] N. Okamura et al., *Prospects of very long base-line neutrino oscillation experiments with the JAERI-KEK high intensity proton accelerator*, `hep-ph/0104220`.

[38] H.W. Zaglauer and K.H. Schwarzer, *The mixing angles in matter for three generations of neutrinos and the MSW mechanism*, *Z. Physik* **C 40** (1988) 273.

JHEP10(2001)001